Materials Science Forum
ISSN: 1662-9752, Vol. 1188, pp 33-44

Submitted: 2026-01-18
Revised: 2026-02-24
Accepted: 2026-02-24
Online: 2026-04-20

RSM-Based Approach to Optimize the Gating System in High Pressure Die Casting

CAMPANELLA Martina[1,a*], PICCININNI Antonio[1,b], CUSANNO Angela[1,c], GUGLIELMI Pasquale[3,d], PALUMBO Gianfranco[1,e], DURACCIO Matteo[2,f] and LEMBO Felice[2,g]

[1]Politecnico di Bari, Italy [2]Master Italy srl, Italy [3]Università degli Studi della Basilicata, Italy

[a*]m.campanella12@phd.poliba.it, [b]antonio.piccininni@poliba.it, [c]angela.cusanno@poliba.it, [d]pasquale.guglielmi@unibas.it, [e]gianfranco.palumbo@poliba.it, [f]m.duraccio@masteritaly.com, [g]f.lembo@masteritaly.com

Keywords: HPDC, Air Entrainment, Response surface methodology, Optimization.

Abstract. High-Pressure Die Casting (HPDC) processes are often affected by complex thermo-fluid-dynamic phenomena that lead to casting defects and premature die degradation. In this study, an approach based on the Response Surface Methodology (RSM) is proposed to improve the quality of the cast part (aluminum window brackets**)** and extend the dies' service life by introducing limited modification to the geometry of the die cavities.

A multi-physics numerical model was initially built up to reproduce the filling and thermal behavior of the process. Infrared thermography, used to validate the numerical results, confirmed the accuracy of the model, with an average temperature error of approximately 2%. The analysis revealed that the baseline configuration (i.e. the dies' geometry currently adopted in the industrial process) was characterized by non-negligible thermal imbalances (temperature gradients of about 50 °C and localized hot spots associated with high melt velocities), which reflected in the occurrence of flashes, metallization, and impression pad damage.

New die geometries with the aim of improving the thermal uniformity while reducing the temperature gradients were investigated by varying the geometrical properties of the gating system according to a DoE-based approach. The numerical results, collected in terms of total amount of porosity in the casting critical areas, were used to train accurate metamodels that, in turns, were adopted as the starting base for a multi-objective optimization. Results from the optimization allowed to identify different scenario, each characterized by a specific geometry of the gating system able to remarkably reduce the occurrence of porosity in the cast part (up to 42% less than the current condition). The results demonstrate that the proposed methodology enables effective and sustainable optimization of HPDC processes without costly trial-and-error approaches.

Introduction

High-pressure die casting (HPDC) is one of the most widely adopted manufacturing processes for the large-scale production of aluminum components with complex geometries and tight dimensional tolerances. Thanks to its high productivity and repeatability, HPDC is extensively used in the automotive and building sectors; however, the process is inherently affected by severe thermal and mechanical loads that strongly influence both casting quality and die service life [1, 2].

During each production cycle, molten aluminum is injected into the die at high velocity and pressure, followed by rapid solidification and cyclic die opening and closing. These conditions generate non-uniform temperature fields within the die, leading to localized hot spots, steep thermal gradients, and differential thermal expansion between die components. Such phenomena are widely recognized as primary causes of casting defects—including porosity, flash formation, soldering, and incomplete filling—as well as premature die wear and surface degradation [3–5].

Among the various process-related issues, thermal imbalance in the gating and runner system plays a critical role. Localized overheating and high melting velocities in these regions can promote air entrapment, metallization, and accelerated degradation of critical die features. Traditional

countermeasures often rely on extensive die redesigns or advanced cooling solutions, which can be costly and difficult to implement in existing industrial production lines.

In this context, computer-aided engineering (CAE) solutions have emerged as powerful tools for understanding the complex thermo-fluid-dynamic behavior of the HPDC process and for supporting process optimization without relying on trial-and-error approaches. In particular, the integration of numerical simulations with Design of Experiments (DoE) and Response Surface Methodology (RSM) enables a systematic exploration of the design space, allowing the influence of multiple geometric and process parameters to be quantified efficiently [6, 7].

In the present work, a simulation-driven methodology is applied to an industrial HPDC process for the manufacturing of aluminum window brackets. Early life defects observed during production motivated the development of a high-fidelity numerical model of the process. Once created the FE model according to the real process and validated against experimental temperature measurements, a modified gating system based on a closed casting configuration was proposed. A DoE-based approach combined with response surface modeling is then employed to optimize the geometry and position of flow-regulating bottlenecks, with the objective of reducing porosity in critical regions of the casting. The study demonstrates how a combined CAE–RSM–optimization framework can improve process stability and die durability through low-impact, cost-effective design modifications[5, 8].

Materials and Methods

Industrial case study and problem description. This study investigates the high-pressure die casting (HPDC) of aluminum window brackets, selected as an industrial case study due to their structural role within window frame assemblies. These components ensure the mechanical connection between frame profiles and are therefore critical for the dimensional stability and durability of the window system.

The brackets are produced on a cold-chamber HPDC press (OMS550), characterized by a closing force of 5,600 kN and a maximum injection force of 520 kN, with an annual production target of approximately 500,000 units. The die is designed as a multi-cavity system and allows the simultaneous production of two different bracket geometries—referred to as male and female components—which are subsequently assembled together by means of a bolt, as shown in Fig. 1.

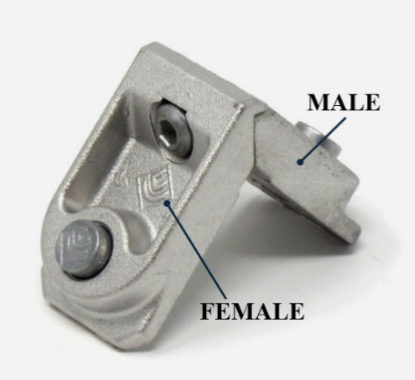

Fig. 1 Two assembled Aluminum widow brackets

The HPDC process follows a well-defined operational sequence with a total cycle time of 34.2 s. Filling and solidification are completed within approximately 10 s to ensure adequate cooling before part ejection. After die opening, the cast parts are removed by a robotic arm, while lubrication and air-blowing operations are performed to prepare the die for the subsequent cycle.

Despite the die being designed for long service life, visual inspections carried out after approximately 2,000 production cycles – corresponding to about 1% of the expected die lifetime – revealed the presence of several critical defects affecting both the cast parts and the die. On the casting side, flashes were observed along the parting lines, as shown in Fig.2. These defects are caused by molten aluminum leakage under high pressure and require additional deburring operations, leading to increased production time and costs.

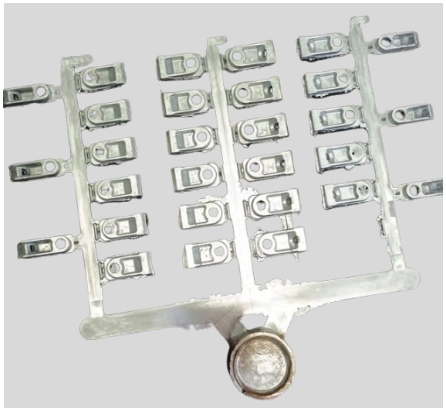

Fig. 2 Final cast part: flashes are evident close to the brackets

In addition, significant degradation phenomena were identified on the die surfaces. As illustrated in Fig.3, lighter regions correspond to areas affected by aluminum adhesion (metallization), resulting from the combined mechanical and chemical interaction between molten aluminum and the die. Over repeated cycles, aluminum build-up alters the local thermal behavior, degrades surface finish, and accelerates die wear. The use of a solvent-based release agent (Chem-Trend #8802), although effective in reducing thermal shock, was found to be less effective in preventing residue accumulation.

Fig. 3 Metallized regions on the die surface

Finally, crushed impression pads were detected in localized regions of the die, particularly near small geometric features, as shown in Fig.4. These defects are associated with the combined action of cyclic thermal fatigue and high mechanical loads. Repeated thermal expansion and contraction promote microcrack initiation and progressive plastic deformation, a phenomenon further intensified during the HPDC intensification phase due to the extremely high internal pressures acting on the die.

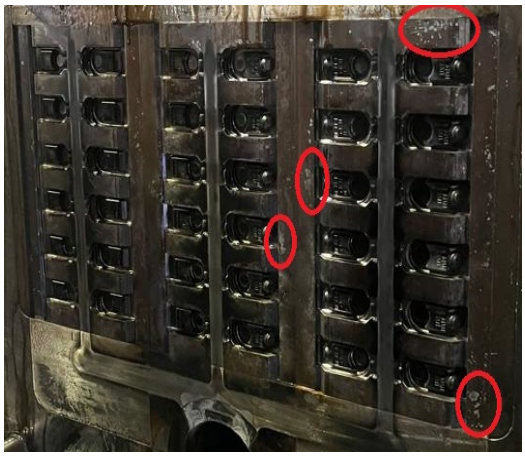

Fig. 4 Defect on the die surface: crushed impression pads on the surface of the die

Numerical simulation of the HPDC process. To investigate the HPDC process in depth, identify the root causes of the observed defects and evaluate effective corrective actions, a numerical modeling strategy based on multi-physics simulations was adopted. The simulations were performed using the commercial finite element software CASTLE, specifically developed for High-Pressure Die Casting applications and capable of coupling fluid-dynamic and thermal analyses within a unified framework. Both Computational Fluid Dynamics (CFD) and Finite Element Method (FEM) solvers were employed to capture the complex thermo-fluid behavior of the process throughout the entire casting cycle. Once calibrate the FE model, two main aspects could be addressed: (i) the fluid flow analysis provided a detailed visualization of the cavity filling, allowing a precise identification of the regions more exposed to shrinkage porosity problems, oxide formation, air entrapment, and misruns; (ii) the thermal analysis identified hot spots, non-uniform cooling, and steep thermal gradients, which have a marked influence on the thermal fatigue, metallization, and impression pad degradation. The CAD geometry of the die, gating system, casting, and cooling channels were imported in STEP format and discretized using a hybrid meshing strategy. Hexahedral elements were employed in the bulk regions of the die, while finer tetrahedral and prismatic elements were adopted in geometrically and physically critical areas, including thin sections, ingates, runners, impression pads, and cooling channels. Mesh refinement was defined to ensure an adequate resolution of local phenomena, with smaller element sizes applied in regions characterized by high thermal gradients and strong fluid–structure interactions. The final computational mesh consisted of approximately 12 million elements.

Material properties for both the casting alloy (EN46100, AlSi11Cu2Fe) and the die material (H13 with Aluminum Coating), were directly selected from the software internal material database. Some of the EN46100 properties accessible by the operator are listed in Table 1.

Table 1 List of properties of the EN46100, AlSi11Cu2Fe alloy (internal library of the CASTLE software)

Property	Value
Density (liquid phase)	2460 [kg/m^3]
Density (solid phase):	2657 [kg/m^3]
Latent heat of solidification:	514,989 [J/kg]
Thermal conductivity (solid phase):	143.2 [W/m·K]
Thermal conductivity (liquid phase)	61.8 [W/m·K]
Liquidus temperature	863 [°C]
Solidus temperature	798 [°C]

Process boundary conditions, including the plunger velocity profile, injection pressure, cycle timing, and cooling strategy, were defined according to the actual industrial operating conditions. The

numerical simulations were carried out over multiple consecutive 15 HPDC cycles in order to capture the initial transient warm-up phase and reach thermal steady-state conditions. During the simulations, the heat transfer coefficient between the cooling water and the die surfaces was not imposed as a constant value but internally estimated as a function of coolant flow rate, channel geometry, and water temperature, ensuring a realistic representation of the heat exchange mechanisms.

Design of the new gating system. Once calibrate the FE model, the geometry of the die cavity was redesigned in order to overcome the limitation of the current solution. Two routes were investigated: (i) closing the gating system in the top part of the die while keeping the same cross section and (ii) introduce bottlenecks in the gating system to choke the flow.
The former solution is visually reported in Fig. 5 where the modification of the cavity is clearly evident.

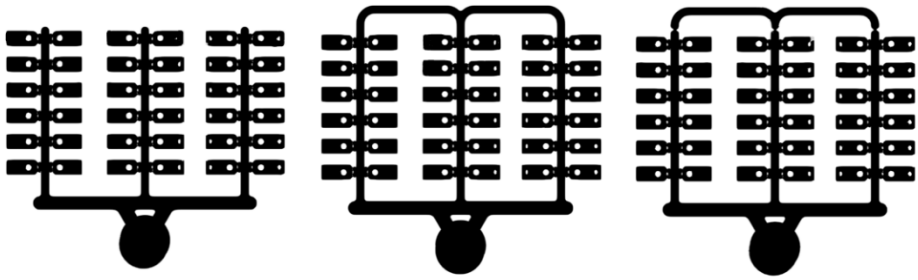

Fig. 5 Comparison between the current configuration, the proposed one (i) and configuration with bottlenecks (ii)

As for the latter aspect, the aim was to optimize the use of the bottlenecks by univocally identifying their geometry and position according to three main parameters. In particular: (i) the parameter L (Fig. 6a) refers to the width of the bottleneck, (ii) the parameters H (Fig. 6b) refers to its height and (iii) the parameter pos identifies the position (Fig. 6c reports simultaneously three possible positions).

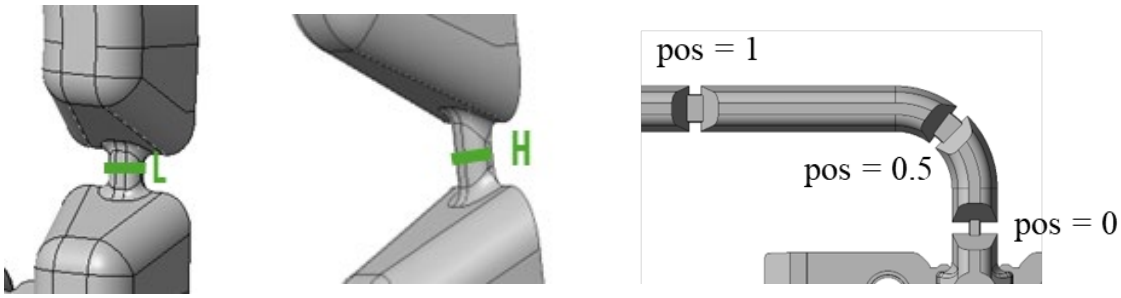

(a) (b) (c)

Fig. 6 Identification of the three main parameters univocally identifying the restriction of the gating system: a) width L, b) height H and c) location pos

Optimization of the bottleneck started from the definition of an ordered plan of numerical simulation, arranged according to a Central Composite Design while varying the three introduced main parameters within the interval ranges reported in Table 2 (possible values of the parameter pos are expressed in a normalized form, where 0 refers to a position of the bottleneck close to the brackets).

Table 2 Variation ranges of the identified input parameters

	L [mm]	H [mm]	Pos [-]
Lower Bound	1	3	1
Upper Bound	9.15	12	0

The distribution of the 15 designs within the design space is graphically reported in Fig. 7a. For each simulation, the casting quality was evaluated by focusing on the most critical geometrical regions, identified based on both industrial feedback and preliminary numerical analyses. Therefore,

two descriptive response variables were defined: (i) the total Air Porosity of the first row of brackets (grouped by the violet box in Fig. 7b), labelled as AP_row1 and (ii) the total Air Porosity of the middle branch of brackets (grouped by the green box in Fig. 7b), labelled as AP_mc. The Fig. 7b corresponds to the alpha1 field (air volume fraction), re-parameterized with respect to the maximum pressure available during the third phase of the injection cycle, and filtered using a 5% air threshold. This representation was adopted to allow a more objective and consistent comparison among different simulation configurations, independently of local pressure fluctuations. The response variables AP_row1 and AP_mc represent the total entrapped air volume integrated over the selected regions of interest (ROIs). Entrapped air was quantified from the CFD scalar field α_1, corresponding to the local air volume fraction. After applying a 5% air threshold to ensure consistent comparison among simulations, the total air porosity in a region Ωwas computed as:

$$AP = \int_{\Omega} \alpha_1 \, dV$$

The resulting value (m^3) represents the total entrapped air within the ROI, providing a continuous and physically consistent measure rather than a binary classification.

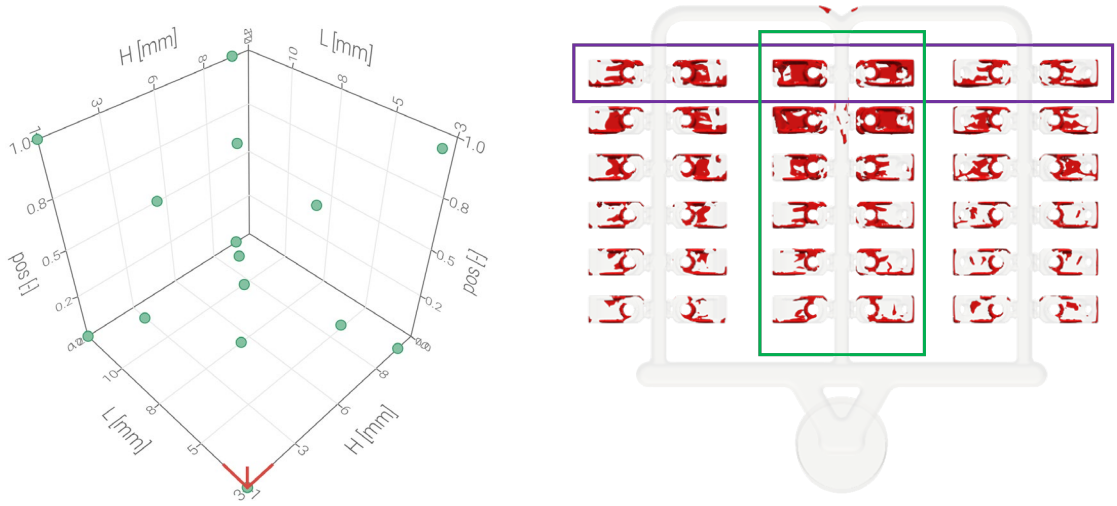

(a) (b)

Fig. 7 RS-based design of the bottlenecks: a) graphical representation of the CCD plan, b) identification of the output response

Data collected from the 15 simulations in terms of the mentioned parameters were subsequently fitted by an interpolating anisotropic Kriging algorithm. The so-trained metamodels (one for each response variable) were subsequently used as the base for a virtual optimization managed by a multi-objective genetic algorithm (MOGA-II). The MOGA, using its main genetic operators, evolved through 1000 virtual generations with the aim of determining the best values of the input parameters to reduce the porosity in the most critical areas (i.e., minimize both AP_row1 and AP_mc).

Results and Discussion

Model validation and root cause analysis. The results from the thermal model were analyzed in terms of temperature distribution along four linear paths, two per die, as shown in Fig. 8. The average temperature calculated for each single path revealed not only a pronounced non-uniform temperature distribution over the die surfaces (with gradient along the vertical direction of around 50°C) but also between the two dies.

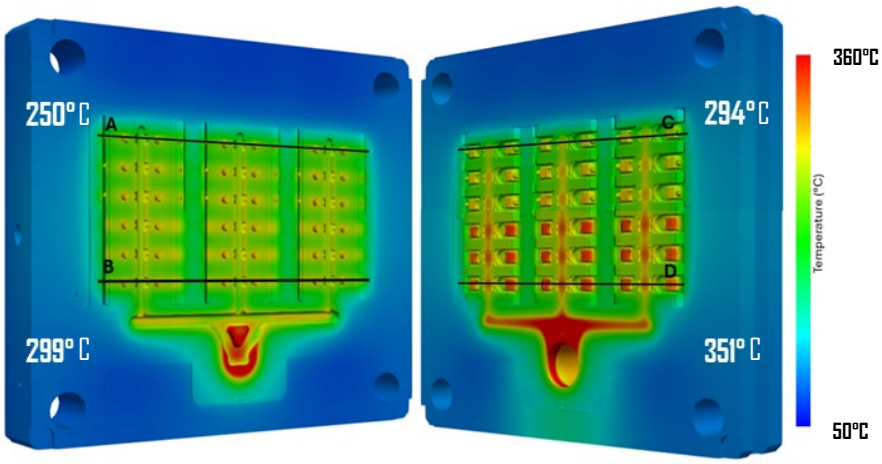

Fig. 8 Surface temperature distribution (before spraying the lubricant) over the movable (left) and fixed (right) die once reached the steady-state condition. Lines A–D indicate the paths along which the temperatures were monitored.

The numerical results were compared with the experimental acquisition (FLIR T6xx infrared thermography): Fig. 9 shows the distribution of the temperature at the 15th cycle immediately before the lubrication and air-blowing phases, along with the average values calculated along the same path investigated in the numerical simulation.

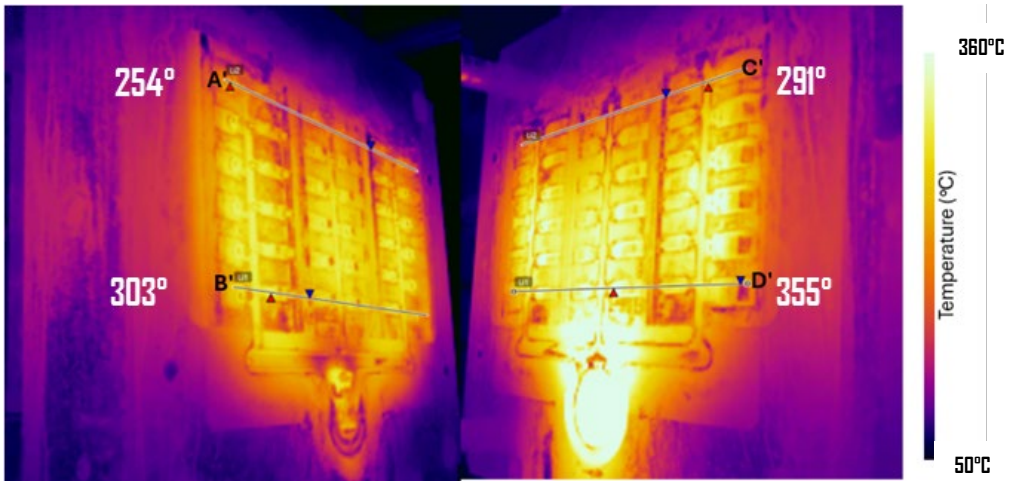

Fig. 9 Infrared thermography of the movable (left) and fixed (right) dies, showing surface temperature distribution at steady-state condition (time instant before the spraying step). Lines A′–D′ indicate the paths along which the temperatures were monitored.

The comparison between numerical predictions and experimental measurements confirmed the accuracy of the FE model, with an average temperature discrepancy of approximately 6 °C (average error of about 2%).

The non-negligible thermal gradient, extremely visible from both the simulation and the experimental acquisition, led to differential thermal expansion, which was directly associated with dimensional instability, flash formation, and premature die degradation. Moreover, localized hot zones were identified in proximity to the central runner and injection area, with peak temperatures reaching up to approximately 350 °C. CFD results shown in Fig.10 further showed that these regions are characterized by very high melt velocities, locally approaching 80 m/s, providing a clear explanation for the metallization phenomena observed on the die surfaces.

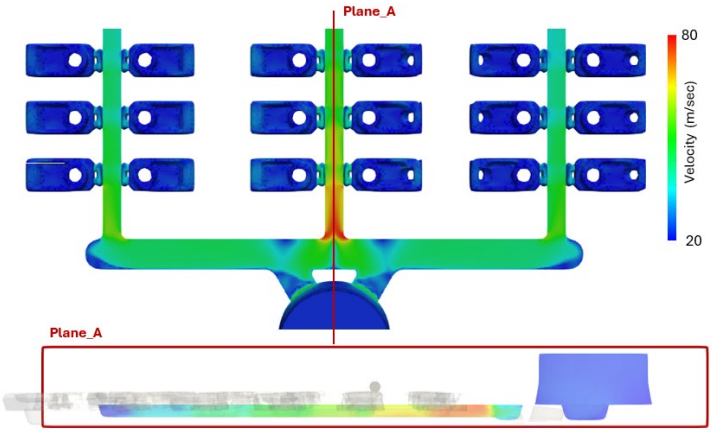

Fig. 10 Simulation of die cavity filling with a particular focus on the velocity distribution in the central runner (the detailed view reports the distribution along the Plane_A cross section)

Gating system redesign strategy. The thermal response of the die after the closure of the gating system in the upper part was analyzed by comparing the surface temperature distributions obtained before the spraying step at steady-state conditions. As shown by the contour plots in Fig. 11, the modification of the die cavities had a marked effect on the thermal behavior of the system, leading to a significantly more uniform temperature distribution compared to the baseline configuration.

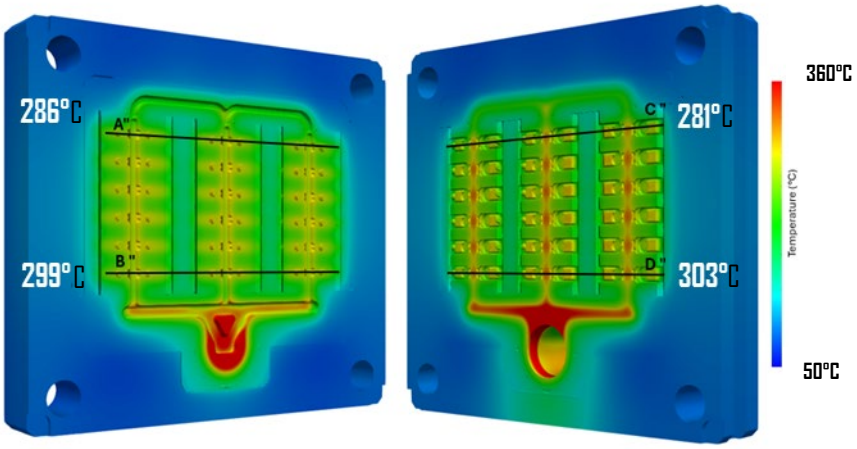

Fig. 11 Closing-casting configuration: Surface temperature distribution (before spraying the lubricant) over the movable (left) and fixed (right) die once reached the steady-state condition (after the 15th cycle). The temperatures were monitored along lines A”–B” and C”–D”.

In particular, the temperature fields on both the movable and fixed dies appear considerably homogenized, with a clear reduction of localized hot regions previously observed in proximity to the runner and injection area. This confirms that the closed gating configuration effectively redistributes the thermal load over the die surfaces.

In line with the analysis presented in Fig.8, temperature profiles were evaluated along the same four horizontal paths (A″ and B″ on the movable die, C″ and D″ on the fixed die). The temperature distributions show a substantial reduction of the vertical thermal gradient. Quantitatively, the temperature difference between the upper and lower regions of the movable die was reduced to 12.6 °C, while a gradient of approximately 22 °C was measured on the fixed die.

These results demonstrate that the closure of the gating system provides a strong thermal stabilization of the die, reducing temperature gradients by more than 50% with respect to the original configuration. Such an improvement is expected to significantly mitigate differential thermal expansion effects, thereby contributing to enhanced dimensional stability and reduced susceptibility to thermally driven die degradation mechanisms. Nevertheless, the remarkable reduction of the thermal imbalance was not accompanied by an equally effective reduction of the bracket porosity, as

shown in Fig. 12: therefore, including the bottlenecks and optimizing their position/geometry was considered necessary to satisfy both the requirements (reduction of porosity and improvement of the material flow).

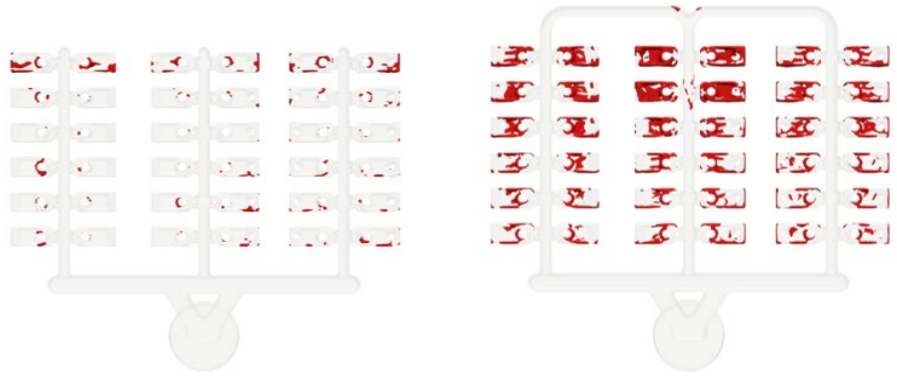

Fig.12 Total porosity distribution: a) current configuration; b) proposed geometry with the closing gating system

Response surface. The trained metamodels are visually represented by the Response Surfaces in Fig. 13, from which interesting considerations could be drawn. In particular, regardless of the specific critical area, it is clear that if the height of the bottleneck is reduced close to the lower bound, its position has almost a negligible effect on the occurrence of the total porosity (see Fig. 13b and Fig. 13d). Moreover, all the reported response surfaces suggest that keeping the height of the bottleneck (H) in a range between 6 and 8 mm is extremely detrimental for the occurrence of porosity (red zones of the response surface). Eventually, it could be also said that the parameter H seems to have a more pronounced effect than the parameter L on the total porosity of both the critical areas.

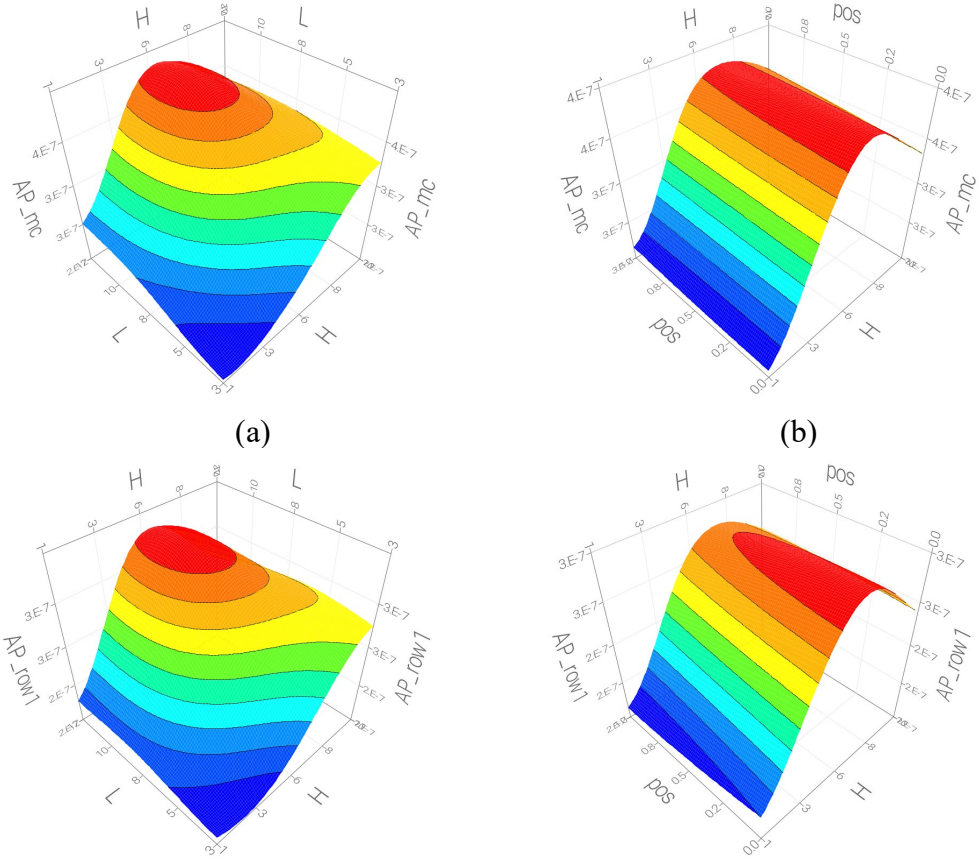

(a) (b)

(c) (d)

Fig. 13 Representation of the trained metamodels on the output variables: (a) and (b) AP_mc; (c) and (d) AP_row1

Optimization results. The main advantage of RS-based optimization is its virtuality: the metamodel is a reliable base from which the MOGA virtually extrapolates designs while trying to satisfy the objective functions. Therefore, the computational cost of the optimization is extremely limited and the number of successive generations can be largely increased: in the present work, 1000 generations were created and the algorithm evolved through 15000 designs. When dealing with a multi-response optimization, it is more likely to face a front of optimal solutions (rather than a unique optimum as it happens with the single objective optimization). Therefore, the Pareto front, defined as the group of non-dominated designs, could be easily extracted from the optimization results and analyzed using the parallel coordinate charts: in this type of charts, all the variables (input and response) are represented by equally spaced parallel vertical lines, whereas each design is represented as a polyline connecting vertices on the vertical axes. By filtering the results, i.e. by specifying a sub-range of the variable values, two distinct optimal scenarios could be spotted.

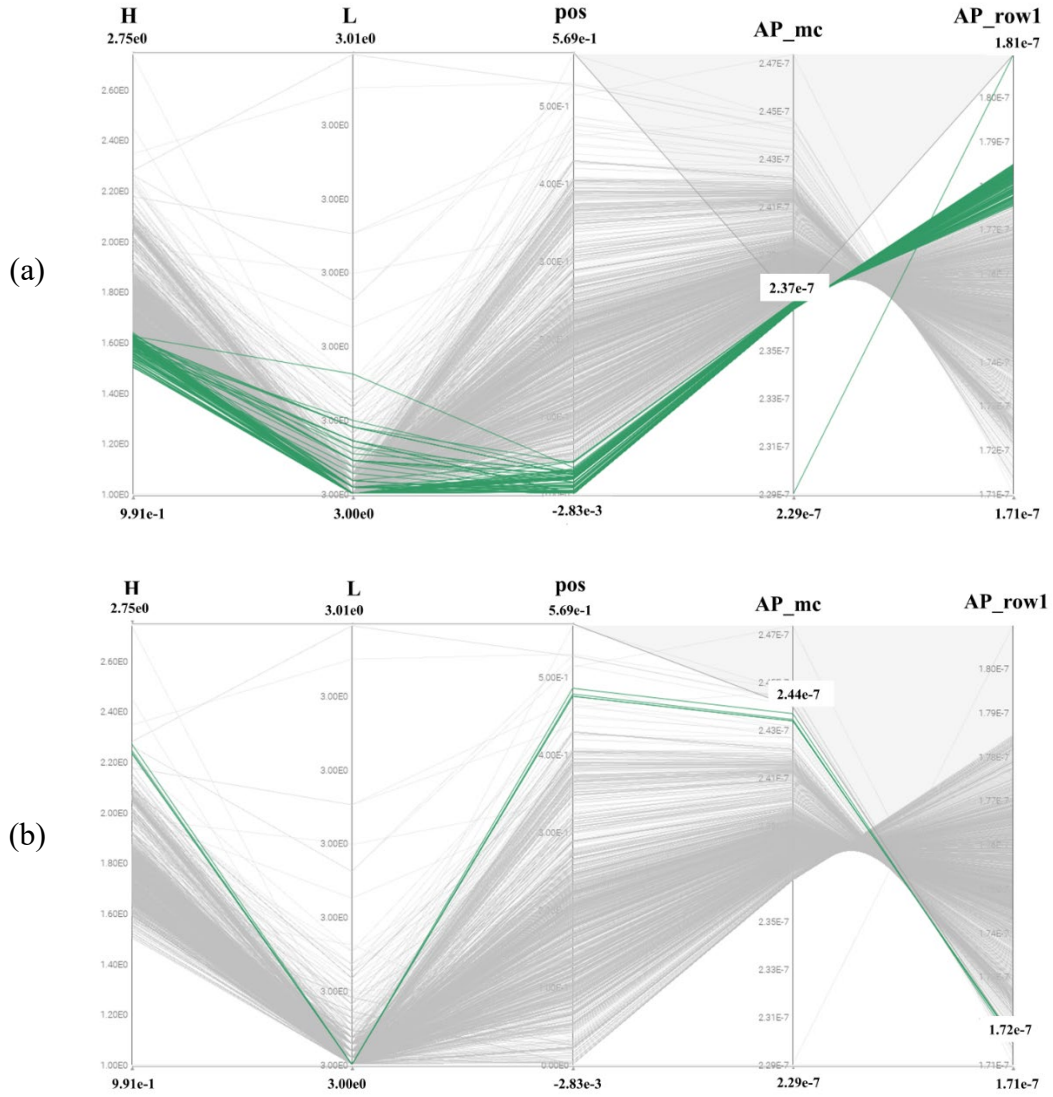

Fig.14 Filtered parallel coordinate charts to identify optimal scenarios: (a) minimization of the AP_mc response and (b) minimization of the AP_row1 response

In fact, as shown in Fig. 14a, if privileging the minimization of the porosity in the middle branch (AP_mc), the bottleneck has to be located as close as possible to the brackets and its geometry characterized by a pronounced restriction in the width (L close to 3 mm) and moderate restriction along the height (H close to 1.5/1.6 mm, slightly higher than its lower bound). On the other hand (see Fig. 14b), the minimization of the porosity of the first row requires again an evident restriction along

the width, but in combination with a less sever reduction of the cross section along the height (H close to 2.2 mm) while locating the bottleneck slightly farther from the brackets (pos close to 0.5 mm).

These results clearly indicate that the optimal design parameters depend on which critical region is prioritized, confirming the presence of a trade-off between the two objectives. Consequently, more than one optimal condition can be identified along the Pareto front, rather than a single global optimum. The two best designs (each minimizing one objective function) were therefore compared with the reference condition (represented by the closed gating system in absence of bottlenecks) in terms of overall porosity, as listed in Table 3.

The optimization was deliberately formulated as a multi-objective problem, maintaining AP_mc and AP_row1 as independent response variables. This choice allows the trade-off between the two critical regions to be explicitly captured and provides a flexible decision-making framework, avoiding the information loss that would result from collapsing the problem into a single averaged objective function.

Table 3 Optimization results: optimal scenarios vs the reference condition

	H [mm]	L [mm]	pos [-]	AP_mc	AP_row1
Reference	9.15	12	/	4.25e-7	2.9e-7
Opt#1	2.7	3	0.5	2.46e-7	1.71e-7
Opt#2	1.5	3	0	2.37e-7	1.78e-7

Summary

In this work, a comprehensive numerical and optimization-based methodology was developed and applied to improve the quality and durability of High-Pressure Die Casting (HPDC) components, with specific reference to aluminum window brackets produced in an industrial environment. A validated multi-physics numerical model of the HPDC process was shown to be an effective and tool for identifying the root causes of premature die degradation and casting defects. The combined CFD–thermal analysis revealed a pronounced thermal imbalance in the currently-adopted configuration, characterized by vertical temperature gradients of approximately 50 °C between the upper and lower regions of the dies. These gradients reflected directly in a differential thermal expansion, flash formation, impression pad crushing, and metallization phenomena, further exacerbated by localized hot spots (up to ~350 °C) and high melt velocities (approaching 80 m/s). A cost-effective and low-impact Closed Casting strategy was numerically investigated as a first corrective action. This modification significantly improved the thermal behavior of the system, leading to a marked homogenization of the temperature field. In particular, the vertical temperature gradient was reduced to 12.6 °C in the movable die and approximately 22 °C in the fixed die, corresponding to an overall reduction exceeding 50%. Such thermal stabilization is expected to substantially mitigate thermally driven die wear mechanisms and improve dimensional stability. Nevertheless, the occurrence of porosity sensibly worsened. Therefore, the implementation of bottlenecks was optimized (in terms of positioning and geometry) by means of an RSM-based optimization. Porosity extracted from a set of simulations (arranged according to a CCD plan) were fitted by anisotropic Kriging metamodels showing the more pronounced effect of the restriction along the height rather than its length on the reduction of porosity. The multi-response optimization, driven by a multi-objective genetic algorithm, enabled the identification of two distinct possible optimal scenarios were identified, each targeting porosity reduction in the most critical regions of the casting. Compared to the reference configuration, the optimized solutions achieved porosity reductions of up to 42% in the middle branch and approximately 39–44% in the first row of brackets. Overall, the proposed methodology demonstrates that combining high-fidelity numerical modeling with DoE-driven, response surface–based optimization allows effective process improvement without costly hardware modifications or trial-and-error approaches. The approach is robust, scalable, and well suited for thin-walled HPDC components, offering a valuable tool for improving casting quality while extending die service life in industrial applications.

References

[1] Handbook of Metal Forming, edited byKurt Lange, Professor, University of Stuttgart (McGraw-Hill, 1985, $85.00; ISBN 0-07-036285-8). Reviewed by Serope Kalpakjian, Professor of Mechanical Engineering, Illinois Institute of Technology.

[2] Dou K, Lordan E, Zhang YJ, et al (2020) A complete computer aided engineering (CAE) modelling and optimization of high pressure die casting (HPDC) process. J Manuf Process 60:435–446. https://doi.org/10.1016/j.jmapro.2020.10.062

[3] Podprocká R, Malik J, Bolibruchová D (2015) Defects in High Pressure Die Casting Process. Manufacturing Technology 15:1–1. https://doi.org/10.21062/UJEP/X.2015/A/1213-2489/MT/15/4/674

[4] Campbell J (2015) Complete Casting Handbook: Metal Casting Processes, Metallurgy, Techniques and Design: Second Edition. 1–1028

[5] Rocha SB, Zhiltsova T, Neto V, Oliveira MSA (2022) Optimization to Assist Design and Analysis of Temperature Control Strategies for Injection Molding—A Review. Materials 15:. https://doi.org/10.3390/ma15124048

[6] Chelladurai SJS, K. M, Ray AP, et al (2021) Optimization of process parameters using response surface methodology: A review. Mater Today Proc 37:1301–1304. https://doi.org/https://doi.org/10.1016/j.matpr.2020.06.466

[7] Han XW, Chen DP (2012) Numerical simulation life prediction of alu-alloy diecasting dies. Adv Mat Res 472–475:2296–2303. https://doi.org/10.4028/www.scientific.net/amr.472-475.2296

[8] Kotas P, Hattel J (2008) Optimization of die filling in high pressure die cast part using MAGMAsoft. 366–368